Progress In Electromagnetics Research, PIER 79, 23–38, 2008

QUAD RIDGED HORN ANTENNA FOR UWB APPLICATIONS

R. Dehdasht-Heydari, H. R. Hassani, and A. R. Mallahzadeh

Electrical Engineering Department
Shahed University
Tehran, Iran

Abstract—This paper describes a novel design of a dual-polarized ultra wideband horn antenna. Based on a VSWR ≤ 2.6, the bandwidth of the designed UWB horn antenna is from 8–18 GHz, most suitable for radar systems. A new coaxial line to quadruple-ridged waveguide transition and a new technique for tapering the flared section of the horn is introduced to improve the return loss and matching of the impedance, respectively. Results of simulation for VSWR, isolation, gain and radiation pattern of designed horn antenna are presented and discussed.

1. INTRODUCTION

Following the Federal Communications Commission definition (FCC) ultra wideband (UWB) systems can be characterized by either a large relative bandwidth (i.e., larger than 20%) or a large absolute bandwidth (i.e., more than 500 MHz) [1]. UWB antennas are more than 100 years old. Some of the very first antennas were biconical and spherical dipoles which have very good wideband characteristics [1]. Recently, many research has taken place on UWB antennas and its applications. In [2], a compact printed circuit board (PCB) monopole antenna in 2.6–14.3 GHz was presented and its performance through a large amount of simulations and measurement were reported. A new design of broadband hybrid antenna over 8–18 GHz for X-band application was reported in [3]. The antenna structure consists of a dielectric resonator, an intermediate substrate and a microstrip fed slot that with integration of these elements a wide bandwidth response was achieved. A novel modified printed tapered monopole antenna (PTMA) for UWB wireless communication (3.1–10.6 GHz

range) application is reported in [4]. In [5], a microstrip square ring slot antenna (MSRSA) for UWB antenna application is proposed and improved by compaction. By splitting the square-ring slot antenna and optimization of the feed network, the required impedance bandwidth over 3.1–10.6 GHz is achieved. One of the simplest and probably the most widely used microwave antenna is the horn. Horn is widely used as a feed element for the large radio astronomy, satellite tracking and communication dishes, found installed throughout the world [6]. When broadband or ultra wideband (UWB) horn antennas are required, it is well known that ridges in the waveguide transition portion and the flare region are required [7–9].

In [10, 11], an E sectoral horn antenna for broadband application using a double-ridged is provided. Recently, a detailed investigation on 1–18 GHz broadband double-ridged horn antenna was reported in [12]. An improved design of the double-ridged horn antenna was presented by Rodriguez [13] showing that a good single radiation beam is maintained for the entire frequency 1–18 GHz range. Another design of the double-ridged horn antenna in 1–18 GHz range with redesigned feeding section was presented in [14] where several modifications are made in structure of a conventional double ridged guide horn antenna in order to overcome the deterioration of its radiation pattern at higher frequency.

It is well known that in microwave applications and radar systems it is very useful and more popular to use dual-polarizations over an ultra wideband range of frequency. In a previous paper [15], the MFIE technique was used to pursue cut off frequencies solutions of quadruple-ridged waveguide modes. When we apply quadruple-ridged in square waveguide the cut off frequency of the TE11 mode becomes close to the TE10 mode resulting in an increase in bandwidth between the TE10 and TE20L modes [16]. However, to the best knowledge of the authors, a few papers have been reported in the open literature concerning the design of quad ridged dual-polarized horn antennas. In [17] a physically compact quad-ridge horn antenna with dual linearly polarized and a maximum VSWR of 3.5:1 over a 3 to 1 operational bandwidth is described. These characteristics were obtained with an antenna which is approximately 50% smaller than conventional quad ridge designs. Recently, a new dual-polarized broadband horn antenna on the 2–26.5 GHz bandwidth with VSWR < 3.1 was reported in [18] where a novel technique for transition between coaxial line to quadruple-ridged waveguide is introduced to improve the return loss performance of the horn antenna. It is based on semi-spherical cavity that is placed in the back of the waveguide. However, in the last two papers design of the waveguide transition and taper of the ridge in the horn are

not sufficiently described and the VSWR in both papers needs to be improved. Furthermore, the size of the aperture and the overall length in [18] is quite large and semi-spherical cavity at the back of waveguide which is rather difficult to construct is required.

In this paper, based on the quadruple-ridged waveguide the design of a quad-ridged horn antenna with dual polarization is presented. Accordingly, a new waveguide transition structure for the single-mode, the TE10 mode, with low return loss performance and a new technique for taper of the flare section is presented. The proposed quad-ridged horn antenna is simulated with commercially available packages such as CST microwave studio and Ansoft's HFSS in the operating frequency range of 8–18 GHz. Simulated results of the designed antenna such as VSWR, isolation, gain and radiation patterns at various frequencies are provided.

2. ANTENNA CONFIGURATION

Figure 1 shows the configuration of the dual-polarized ultra wide band quad-ridged horn antenna. The overall length of the designed horn is 8 cm with an aperture size of $5.6 \times 5.6\,\text{cm}^2$. The horn antenna is divided into three parts: a quadruple-ridged waveguide, a square shorting plate (cavity back) placed at back of the waveguide, and the flare section of the horn with tapered quadruple-ridges. In the following sections design steps for each of the above sections will be described.

2.1. Design of the Quadruple-ridged Square Waveguide

The waveguide transition of the horn antenna can be divided into two parts: a square quadruple-ridged waveguide and a shorting plate located at the back of the waveguide. The quadruple-ridged waveguide is a square one loaded with four ridges of two orthogonal polarizations. For single-mode operation, increase of the bandwidth between the TE10 and the TE20L modes and impedance matched to the impedance of coaxial cable (50 ohms) can be obtained by loading ridges with a very small gap. In first step, as shown in Fig. 2, we simulated a two ports quadruple-waveguide without coaxial probes for single-mode (i.e., TE10 mode) in the operating frequency range of 8–18 GHz with CST microwave studio. The height and width of the designed ridges are $h = 0.65\,\text{cm}$ and $s = 0.28\,\text{cm}$ respectively that are loaded in a square waveguide shown in Fig. 1. The aperture and overall length of the waveguide are $a = 1.6 \times 1.6\,\text{cm}^2$ and $l = 4\,\text{cm}$, respectively. The S12 parameters of the TE10 and TE20L modes in waveguide versus the frequency are presented in Figs. 3 and 4. Fig. 3 shows that

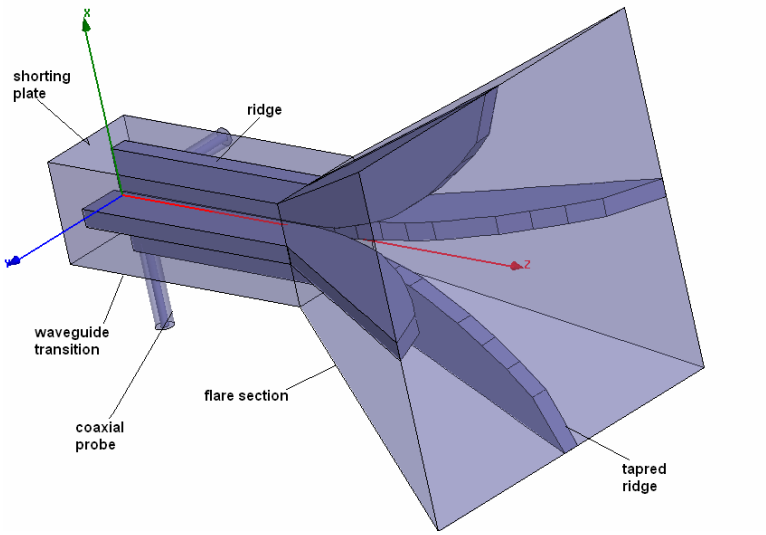

Figure 1. Configuration of the proposed horn antenna.

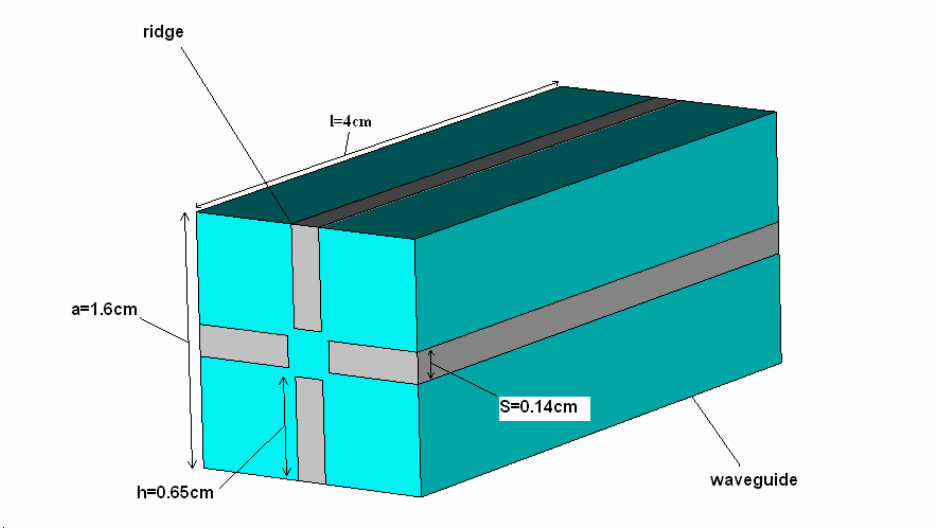

Figure 2. Two ports quadruple-ridged waveguide without coaxial probes.

the lowest mode (i.e., TE10) is the fundamental propagation mode in the waveguide because of it's S12 parameter being approximately 0 dB. TE11 mode is close to the TE10 in cutoff frequency. This fact

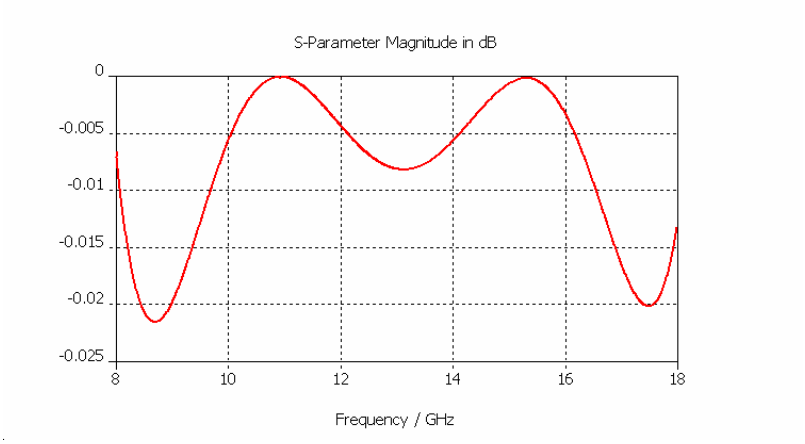

Figure 3. S12 parameter of the TE10 mode versus frequency (propagation mode).

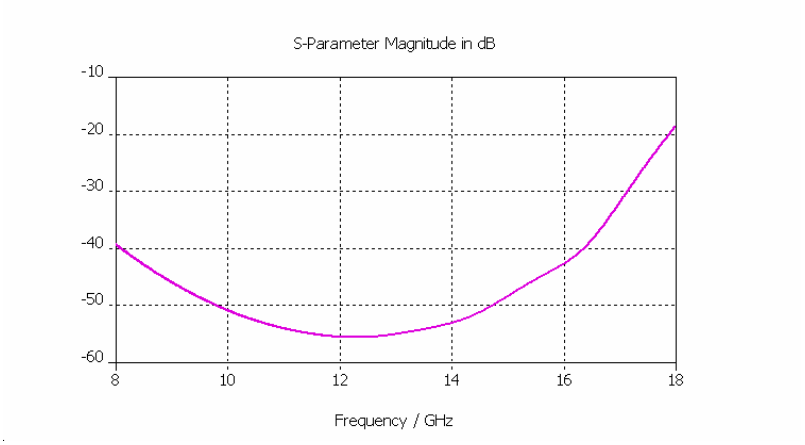

Figure 4. S12 parameter of the TE20L mode versus frequency (non propagation mode).

distinguishes a quadruple-ridged waveguide significantly from a single- or dual-ridged waveguide. However, if the TE11 mode is sufficiently suppressed or not excited the bandwidth between the TE10 and the TE20L can be very large [16]. In Fig. 4, we observe that higher order mode, i.e., TE20L, can not propagate in the waveguide because the S12 parameter is much lower than 0 dB.

In next step, it is necessary to use the transition between two coaxial probes to the quadruple-ridged waveguide. One coaxial probe

for vertical polarization and the other for horizontal polarization. Entrance of the coaxial probes is critical for the return loss performance of the horn antenna. A lot of simulations have been made to optimize the transitional performance using Ansoft's HFSS. In our simulations, we assumed that quadruple-ridged waveguide absorb the full wave that is propagated from coaxial probes. For the good isolation and low return loss, we found that two features are necessary:

(a) The inner conductor of the coaxial probes passes through the first ridges and is then connected to the opposite ridges. This feature is presented in Fig. 5 for coaxial probe entrance to the horizontal ridges in the waveguide transition. Similarly the same technique is used for entrance of the second coaxial probe for vertical ridges that is not shown in Fig. 5.

(b) The inner conductor and shield of the coaxial probes should enter very close to the edge of the ridges. This feature is shown in Fig. 6. As can be seen from this figure, due to the space limits between the two inner conductors of the coaxial probes in the ridges, the horizontal ridge is made to sit slightly back compared to the vertical ridge, the distance between edges of vertical and horizontal ridges being $d = 0.14\,\text{cm}$.

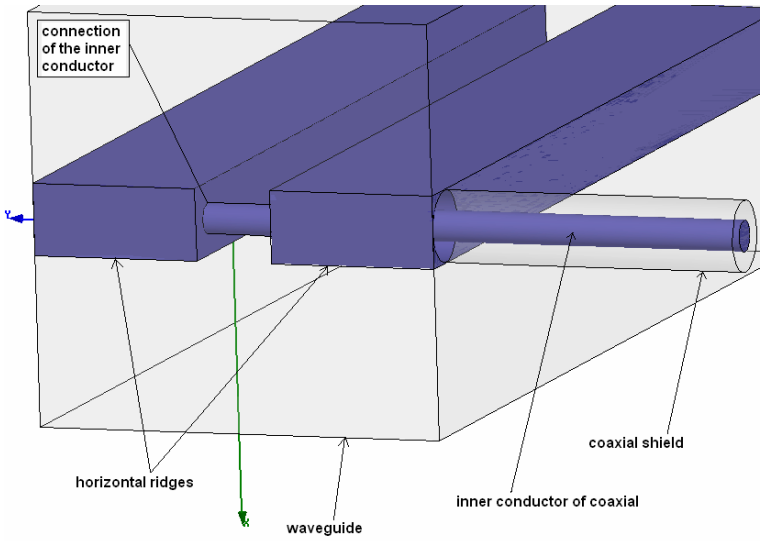

Figure 5. Coaxial probe entrance to horizontal ridges in waveguide transition.

It is very prevalent to use a shorting plate (cavity back) to obtain a much lower return loss in waveguide transitions. A simple square

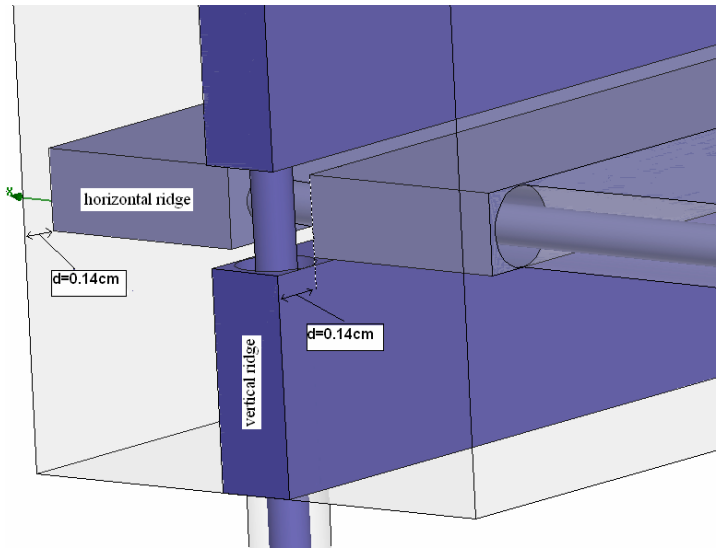

Figure 6. Vertical and horizontal ridges in waveguide transition with coaxial probes.

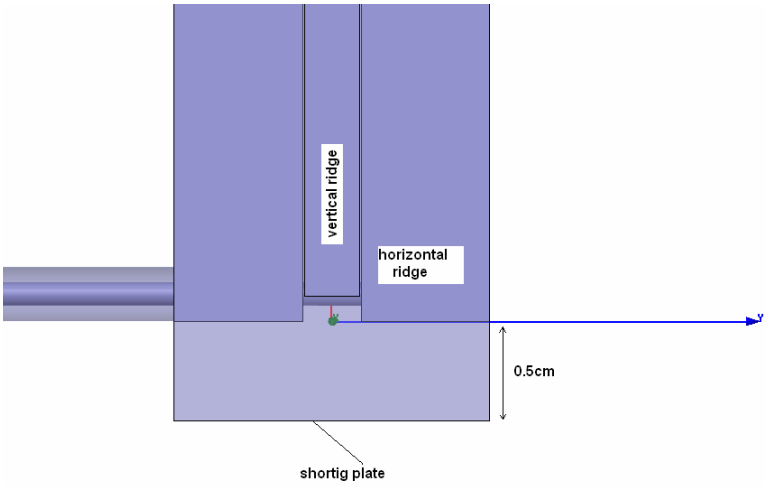

Figure 7. Shorting plate for lower return loss in waveguide transition.

shorting plate is used in this design at the end of the waveguide structure, shown Fig. 7. The space between the end of the waveguide transition to this shorting plate is 0.5 cm.

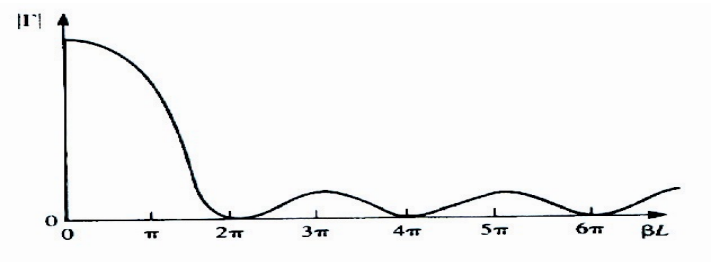

Figure 8. Magnitude of reflection coefficient versus the normalized cutoff wave number βL.

2.2. Determination of the Overall Length and Aperture Size of the Designed Horn

The magnitude of reflection coefficient versus the normalized cutoff wave number for an exponential tapered line as given in [19] is shown in Fig. 8. In this figure, we observe that for low reflection coefficient, βL must be more than 2π. β_c is the cutoff wave number, that can be calculated for the lowest and highest cutoff frequencies of 8 and 18 GHz. L being the overall length of the designed horn and can be determined from $L > \lambda_c$ where $\lambda_c = 2\pi/\beta_c$. For the desired gain, approximately 12–13 dB, over the operating frequency range, aperture size is determined from the simulation of the horn antenna without the ridges. This aperture size is obtained to be $5.6 \times 5.6\,\text{cm}^2$ with L being 4 cm.

2.3. A New Technique for Tapering the Quad-ridged in the Horn

The last step in the design of the antenna is the tapering of the four identical ridges which are of exponential shape. The ridge's height and width must be such that the associated impedance taper is a smooth transition from the waveguide impedance (50 Ω or less) to the free space impedance, 377 Ω [9]. It has been found that an exponential impedance taper of the form [19]:

$$Z = Z_o e^{kx} \quad 0 \le x \le L \tag{1}$$

where Z_o is the characteristic impedance of the waveguide and L is the overall length of the flare section of the horn that was determined in Section 2.2 (with $L = 4$ cm). k is a constant equal to $(1/L)\ln(Z(L)/Z_o)$, with $Z(L)$ being the impedance of the horn at the aperture. To improve the impedance matching between the quadruple-ridged waveguide and the free space, a modified exponential function

can be used [8]:

$$Z = 0.02x + Z_o e^{kx} \quad 0 \le x \le L \tag{2}$$

In the proposed technique, we divide L to some ten sections, each of length 0.4 cm, i.e., we are approximating the overall horn to be made from ten smaller waveguides each with a length of 0.4 cm. The aperture size of each of the smaller waveguides is obtained from the linear flare of the main horn antenna. Then the characteristic impedance of each of the ten smaller waveguides can be obtained from Equation (2), where x would start from 0.4 cm for the first waveguide and increases by o.4 cm for each of the other waveguides. Ten quad-ridged small waveguides with constant width ridges (equal to the width of ridges in transition waveguide) and variable height are simulated with Ansoft's HFSS in order to match the characteristic impedance obtainable from Equation (2). The aperture sizes and characteristic impedances and height of ridges are tabulated in Table 1. After obtaining the height of the ridges we connect them together in the flare section of the horn antenna. The final shape of the ridges appears as exponential taper and is shown in Fig. 9.

Table 1. The aperture size, characteristic impedance and the height of the tapered ridges in the horn antenna.

Waveguide number	**Aperture sizes (cm)**	***Zo* (Ω)**	**Height of tapered ridges (cm)**
1	1.6×1.6	47	0.65
2	2×2	57	0.81
3	2.4×2.4	71.6	0.91
4	2.8×2.8	87.7	1
5	3.2×3.2	108	1.06
6	3.6×3.6	133	1.03
7	4×4	163	1
8	4.4×4.4	201.6	0.91
9	4.8×4.8	248	0.79
10	5.2×5.2	305.6	0.62

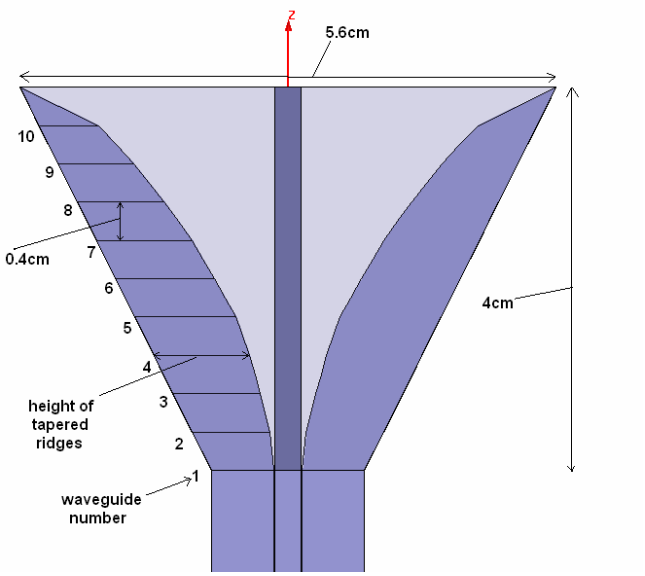

Figure 9. The quad-ridged horn antenna made from ten smaller waveguides each of different height.

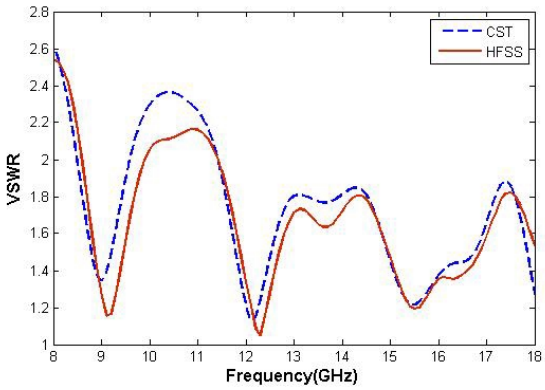

Figure 10. Simulated VSWR of port 1.

3. RESULTS OF SIMULATION

To emphasis on the accuracy of the simulated results, two commercially available software packages, the HFSS and CST have been used. Both show a very close results confirming that the simulated results are obtained with reasonable accuracy.

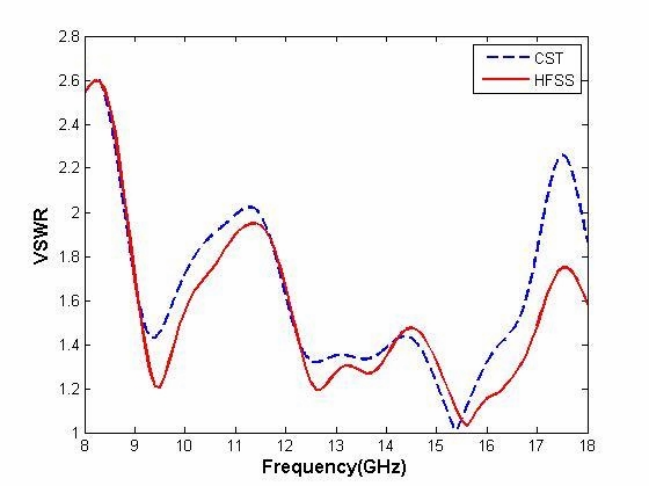

Figure 11. Simulated VSWR of port 2.

The voltage standing wave ratio (VSWR) results of the designed horn antenna are presented in Figs. 10 and 11. It can be seen that both of the coaxial ports have VSWR ≤ 2.6 over the frequency range of 8–18 GHz. From these figures it is obvious that the VSWR initially (around 8 GHz) starts from 2.6 and around 8.3 GHz it reaches below 2.4, i.e., the required band of 8–18 GHz is effectively below VSWR of 2.4. The isolation between the two coaxial ports is shown in Fig. 12 which is better than 19.92 dB over the entire frequency.

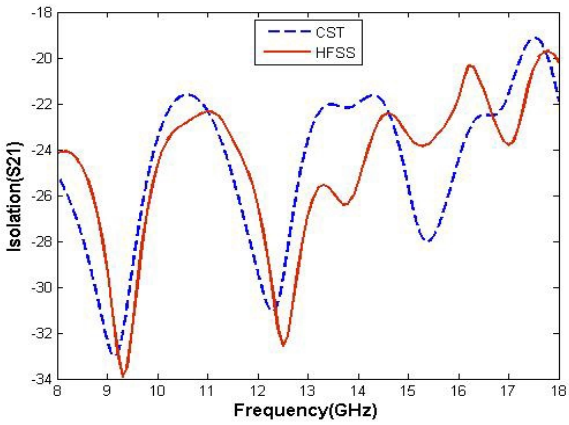

Figure 12. Simulated isolation S12 of the horn antenna.

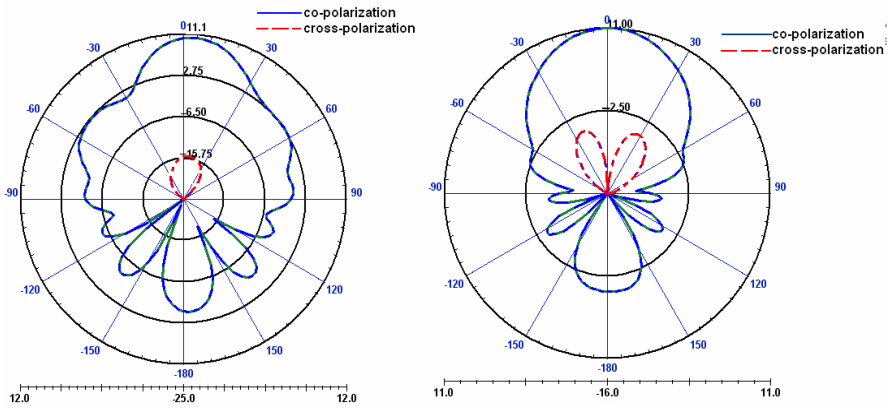

Figure 13. Simulated E- and H-plane patterns at 8 GHz. (a) E-plane, (b) H-plane.

Figures 13–15 show simulated co- and cross polar far-field E- and H-plane radiation patterns at 8, 13, 18 GHz. From these figures it is seen that the cross polar, the back lobe and side lobe level (SLL) are quite low. Table 2 provides the main characteristics of the proposed antenna, such as the SLL and half power beam width (HPBW) in both the E- and H-plane at the 3 different frequencies. The presence of the ridges has not caused any degradation of the field patterns only the required bandwidth is provided. Only at the high frequency, 18GHz, the main beam in the E-plane rotates by some 15 degrees.

Table 2. The main characteristics of the proposed antenna in E- and H-planes.

Frequency (GHz)	HPBW (deg)	SLL (dB)	Plane
8	36.8	−7.5	E
8	56.5	−18.9	H
13	40.1	−11.8	E
13	31	−19.5	H
18	40.4	−8.2	E
18	24.6	−20.8	H

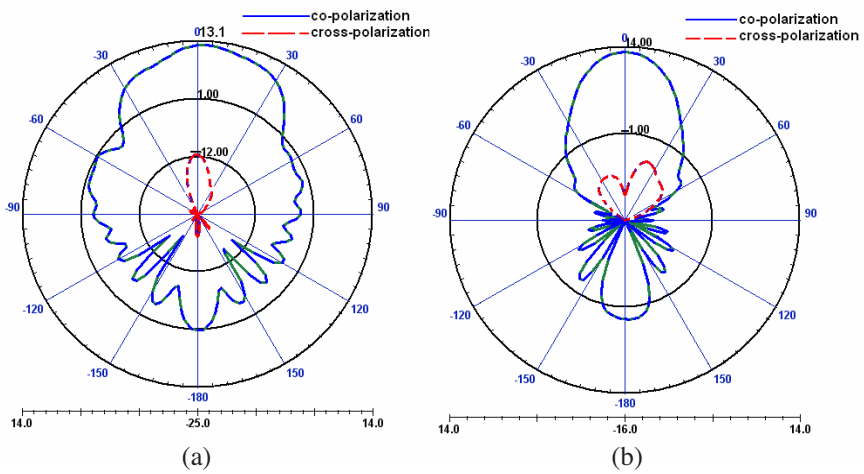

Figure 14. Simulated E- and H-plane patterns at 13 GHz. (a) E-plane, (b) H-plane.

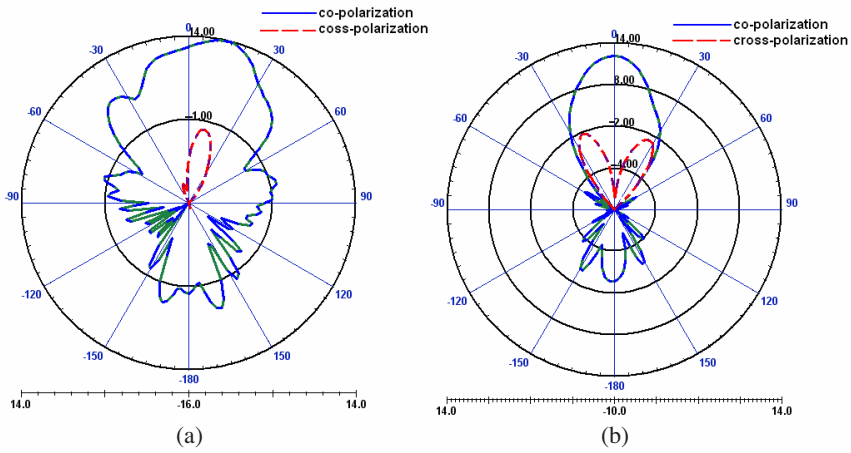

Figure 15. Simulated E- and H-plane patterns at 18 GHz. (a) E-plane, (b) H-plane.

The magnitude of the E-field at center frequency, 13 GHz, in two orthogonal cross sections is shown in Fig. 16 where it is obvious that the presence of the dual polarized feed and the shorting plate at the back of the waveguide has not made any significant changes to the field pattern within the waveguide horn antenna compared to a conventional horn.

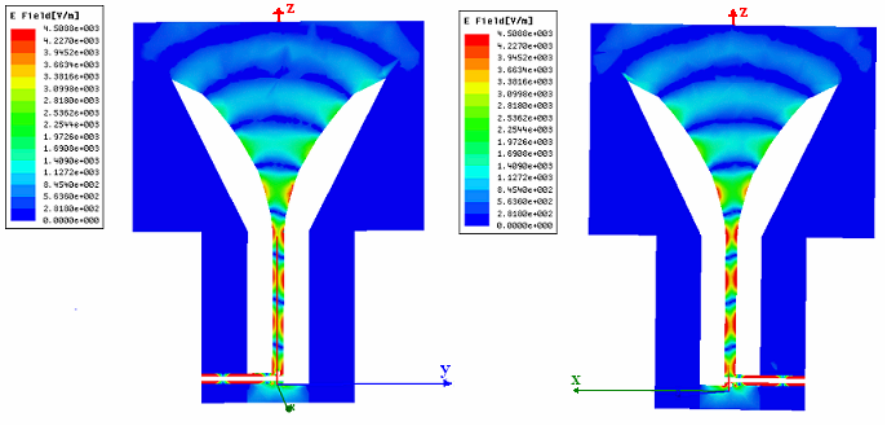

Figure 16. The magnitude of the E-field over two cross sections of the antenna at center frequency 13 GHz.

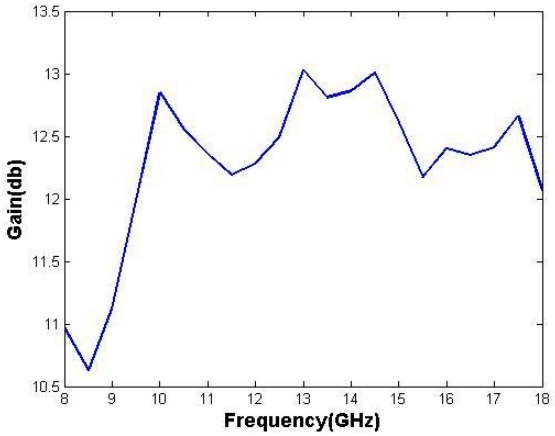

Figure 17. Gain versus frequency for the proposed antenna.

Figure 17 shows the simulated gain of the horn antenna for various frequencies. The result shows that the gain (for theta = 0°) is almost constant over the bandwidth, 10.5–13 dB, and the peak value occurs around the centre frequency of the band. Furthermore, it is found from simulation that the gain and radiation pattern results are almost the same for both horizontal and vertical polarizations.

4. CONCLUSION

This paper has presented a novel design of the dual-polarized ultra wide band quad ridged horn antenna. The simulation of the designed horn antenna has shown good VSWR (1:2.6), isolation (less than 19.92 dB) and gain (10.5–13 dB) results over the ultra wide band frequency of 8–18 GHz. This frequency range along with dual-polarizations is very useful for radar systems and microwave applications.

REFERENCES

1. Allen, B., M. Dohler, E. E. Okon, W. Q. Malik, A. K. Brown, and D. J. Edward, *Ultra-wideband Antennas and Propagation for Communications Radar and Imaging*, 1st edition, John Wiley & Sons, Inc., 2007.
2. Ren, W., J. Y. Deng, and K. S. Chen, "Compact PCB monopole antenna for UWB applications," *Journal of Electromagnetic Wave and Applications*, Vol. 21, No. 10, 1411–1420, 2007.
3. Coulibaly, Y. and T. A. Denidni, "Design a broadband hybrid dielectric resonator antenna for X-band applications," *Journal of Electromagnetic Wave and Applications*, Vol. 20, No. 12, 1629–1642, 2006.
4. Zaker, R., Ch. Ghobadi, and J. Nourina, "A modified microstrip-fed tow step tapered monopole antenna for UWB and WLAN applications," *Progress In Electromagnetics Research*, PIER 77, 137–148, 2007.
5. Sadat, S., M. Fardis, F. Geran, and G. Dadashzadeh, "A compact microstrip square-ring slot antenna for UWB applications," *Progress In Electromagnetics Research*, PIER 67, 173–179, 2007.
6. Balanis, C. A., *Antenna Theory Analysis and Design*, 3rd edition, John Wiley & Sons, Inc., 2005.
7. Cohn, S. B., "Properties of ridged waveguide," *Proc. IRE*, Vol. 35, 783–778, Aug. 1947.
8. Kerr, J. L., "Short axial length broad-band horns," *IEEE Trans. Antennas Propag.*, Vol. AP-21, No. 5, 710–714, Sep. 1973.
9. Walton, K. L. and V. C. Sundberg, "Broadband ridged horn design," *Microwave Journal*, 96–101, Mar. 1964.
10. Reig, C. and E. Navarro, "FDTD analysis of E-sectoral horn antenna for broadband applications," *IEEE Trans. Antennas Propag.*, Vol. 45, No. 10, 1485–1487, Oct. 1997.

11. Bunger, R., R. Beyer, and F. Arndt, "FDTD analysis of E-sectoral horn antennas for broadband applications," *IEEE Trans. Antennas Propag.*, Vol. 47, No. 11, 1641–1648, Nov. 1999.
12. Bruns, C., P. Leuchtman, and R. Vahldieck, "Analysis and simulation of a 1–18 GHz broadband double-ridged horn antenna," *IEEE Trans. Electrmagn. Compat.*, Vol. 45, No. l, 55–60, Feb. 2003.
13. Rodriguez, V., "New broadband EMC double-ridged guide horn antenna," *R.F. Des.*, 44–47, May 2004.
14. Abbas-Azimi, M., F. Arazm, J. Rashed-Mohassel, and R. Faraji-Dana, "Design and optimization of a new 1–18 GHz double ridged guide horn antenna," *Journal of Electromagnetic Wave and Applications*, Vol. 21, No. 4, 501–506, 2007.
15. Sun, W. and C. A. Balanis, "MPIE analysis and design fridged waveguides," *IEEE Trans. Microwave Theory & Tech.*, Vol. 41, No. 11, 1965–1971, Nov. 1993.
16. Sun, W. and C. A. Balanis, "Analysis and design of quadruple ridged waveguide," *IEEE Trans. Microwave Theory & Tech.*, Vol. 42, No. 12, 2201–2207, Dec. 1994.
17. Soroka, S., "A physically compact quad ridged horn design," *IEEE Antenna and Propag. Society International Symposium*, Vol. 24, 903–904, June 1986.
18. Shen, Z. and C. Feng, "A new dual-polarized broadband horn antenna," *IEEE Antenna and Wireless Propag. Letters*, Vol. 4, 270–273, 2005.
19. Pozar, D. M., *Microwave Engineering*, 3rd edition, John Wiley & Sons Inc., 2005.